Membrane and Water Treatment, *Vol. 14, No. 3 (2023) 121-128*
https://doi.org/10.12989/mwt.2023.14.3.121

Selective removal of cationic dye pollutants using coal ash-derived zeolite/zinc adsorbents

Chatchai Rodwihok[1a], Mayulee Suwannakaew[1b], Sang Woo Han[1b], Siyu Chen[1b], Duangmanee Wongratanaphisan[2a] and Han S. Kim[*1]

[1]*Civil and Environmental Engineering, Konkuk University, 120 Neungdong-ro, Gwangjin-gu, Seoul 05029, Republic of Korea*
[2]*Department of Physics and Materials Science, Faculty of Science, Chiang Mai University, Chiang Mai 50200, Thailand*

(Received July 17, 2023, Revised August 20, 2023, Accepted August 21, 2023)

Abstract. This study introduces a NaOH/Zn-assisted hydrothermal method for the synthesis of zeolites derived from coal ash (CA). A zeolite/Zn adsorbent is successfully prepared by the activation of CA with NaOH and Zn; it is characterized by a high surface area and a negative surface charge. Methylene blue (MB) and methyl orange (MO) are selected as dye pollutants, and their adsorption onto the zeolite/Zn adsorbent is investigated. Results show the high adsorption capacities of MB and MO and that the negative surface charge facilitates electrostatic interactions between the adsorbates and adsorbents. The zeolite/Zn adsorbents shows the selective adsorption of positively charged dye MB via electrostatic interactions between the =NH+ group (positive dipole) and the oxygen functional group of the adsorbents (negative dipole). The selectivity for the positively charged dye is sufficiently high, with the removal efficiency reaching 99.41% within 10 min. By contrast, the negatively charged dye MO exhibits negligible absorption. These findings confirm the role of electrostatic interactions in the adsorption of MB, in addition to the effect of a large surface area. The results of this study are expected to facilitate the development of simple, eco-friendly, and cost-effective zeolite-based adsorptive composites from CA residuals for the selective removal of dye pollutants from CA waste.
Keywords: coal ash; surface modification; zeolite; organic dyes; selective adsorption

1. Introduction

Organic dyes pose a significant threat to the environment and living organisms due to their high toxicity and carcinogenicity (Lellis *et al*. 2019). These compounds, which are typically used in textiles, exhibit complex structures and high stabilities, thus rendering them recalcitrant after discharge into natural water bodies (Al-Tohamy *et al*. 2022, Wang *et al*. 2022). Various techniques have been developed to remove dye molecules from wastewater systems, including ion exchange, solvent extraction, filtration, coagulation-flocculation, electrochemical treatment, advanced oxidation processes, and adsorption (David *et al*. 2020, Ihaddaden *et al*. 2022, Januário *et al*. 2021, Joseph *et al*. 2020, Kaur *et al*. 2018, Saruchi and Kumar, 2019). Among these techniques, adsorption is favored as a highly effective removal process because of its simplicity, ease of operation, and minimal generation of residual byproducts (He *et al*. 2019, Molla *et al*. 2019, Rodwihok *et al*. 2023, Zhang *et al*. 2018). Consequently, researchers have focused on identifying new and effective adsorbent materials for the removal of organic dye pollutants.

Recently, zeolites have received significant attention in the area of dye removal via adsorption owing to their high adsorption capacity, excellent chemical stability, and wide availability as a natural resource (Jawad *et al*. 2020, Kazemi and Javanbakht, 2020, Rakanović *et al*. 2022). In particular, the surface modification of zeolites using carbon-based materials and metal/metal oxide additives for adsorption processes in water and wastewater treatment has been investigated (Li *et al*. 2020, Lin *et al*. 2016, Madan *et al*. 2019, Nyankson *et al*. 2020, Rubab *et al*. 2021, Shui *et al*. 2020, Singh *et al*. 2023). Copper can be effectively removed, even at high concentrations (500 ppm), using MnO_2-grafted zeolite, which facilitates electrostatic interactions between copper and zeolite (Balintova *et al*. 2021). The addition of TiO_2 enhances the adsorption capacity of the dyes by increasing the specific surface area of zeolite (Visa *et al*. 2015a). Coal ash (CA) is a representative solid waste generated from coal-fired power plants that challenges the management of industrial waste owing to its large-scale production (Bin *et al*. 2020, Lim *et al*. 2020, Park *et al*. 2021, Rodwihok *et al*. 2021b). Coal ash waste, containing toxic heavy metals such as mercury and arsenic, poses serious health risks including respiratory and cardiovascular issues, cancer, developmental disorders, and contamination of water resources. Proper management and transitioning to cleaner energy are essential to mitigate these health impacts. Despite recycling efforts, most CA waste is currently disposed of in landfill sites, particularly in the case of large-scale disposal (Park *et al*. 2021). CA is primarily comprised of silica, alumina, and iron oxides, along with residual oxides such as calcium, potassium,

[*]Corresponding author, Ph.D., Professor,
E-mail: hankim@konkuk.ac.kr
[a]Ph.D.
[b]Ph.D. Student

ISSN: 2005-8624 (Print), 2092-7037 (Online)

magnesium oxides, and trace amounts of other minerals (e.g., TiO_2, P_2O_5, and SO_3) (Park *et al*. 2021). Owing to its thermal stability, large surface area, electrostatic characteristics, and economic advantages, CA has received significant interest as a valuable raw material for zeolite production (Bin *et al*. 2020, Lim *et al*. 2019, 2020, Park *et al*. 2019, Zol *et al*. 2020). Moreover, CA exhibits high sorptive capacity for heavy metal ions and organic compounds (Li *et al*. 2021, Querol *et al*. 2002, Rodwihok *et al*. 2023).

Herein, we report a new technique for preparing zeolites from CA using a NaOH/Zn-assisted hydrothermal method. The physical and chemical properties of the prepared adsorbents are investigated to assess their interfacial potential for selective dye removal. Owing to the current necessity to minimize disposal, including that from treatment processes (i.e., zero-disposal process), and the demand for eco-friendly and sustainable environmental technologies, the results of this study are expected to contribute to such activities via the introduction of a novel recycling and reuse technique for solid wastes generated from coal-fired power plants.

2. Materials and methods

2.1 Preparation of zeolite/Zn adsorbents

Deionized (DI) water with a volume of 500 mL was mixed with 5 g of CA (fly ash) obtained from the Korea South-Est Power Co., Yeongheung Power Division, South Korea. The mixture was stirred on a shaker table operated at 500 strokes per min at 25 °C for 30 min. A neodymium magnetic bar wrapped with Parafilm was immersed in the prepared solution to remove magnetic components from the CA. The magnetic bar was rinsed multiple times with DI water and immersed in the CA solution until no magnetic components were present. The resulting precipitated fractions were washed five times with DI water after centrifugation at 1,500×*g* for 10 min, and then dried at 80 °C for 24 h. Subsequently, the powdered material was rinsed with 500 mL of 5 M acetic acid (99.7% purity; Samchun Pure Chemical, Gyeonggi, South Korea) for 24 h. The resulting precipitated fraction was washed with DI water and centrifuged at 1,500×*g* for 10 min. Finally, the obtained CA powder was dried at 80 °C for 24 h. Zeolite/Zn adsorbents were synthesized via the following hydrothermal technique: 3 g of washed CA was mixed with zinc acetate dihydrate ($Zn(CH_3COO)_2{\cdot}2H_2O$, 98%, Samchun Pure Chemical, Gyeonggi, South Korea). The mixture was mixed with 60 mL of DI water and stirred on a shaker table operated at 500 strokes/min for 20 min. Subsequently, 50 mL of DI water containing 4 g of NaOH (98% purity; Samchun Pure Chemical, Gyeonggi, South Korea) was added until the pH reached 12. The resulting solution was transferred to a Teflon-lined autoclave container and heated to 160 °C and maintained for 6 h. The resulting product was obtained via configuration, washed five times with DI water, and dried at 80 °C for 24 h to obtain zeolite/Zn adsorbents. The same procedure without the zinc acetate additive was performed to obtain simple zeolite adsorbents.

2.2 Characterization of zeolite/Zn adsorbents

The surface morphologies of the prepared adsorbents were analyzed via field-emission scanning electron microscopy (FE-SEM, SU8010, Hitachi, Japan). The mineralogical composition and phase structure were characterized using X-ray diffraction (XRD, JP/MAX-3C, Rigaku, Japan). Fourier transform infrared (FT-IR) spectroscopy (Thermo Fisher Scientific, Waltham, MA, USA) was performed to analyze the surface functional groups. The specific surface area and pore volume were determined based on the Brunauer–Emmett–Teller (BET) equation using a nitrogen adsorption–desorption BET analyzer (3Flex, Micromeritics, Norcross, GA, USA). The surface charge was measured using a Zetasizer device (Zetasizer Nano ZS, Malvern, Netherlands).

2.3 Efficiency of MB and MO adsorption by zeolite/Zn adsorbents

To assess dye adsorption, methylene blue (MB) and methyl orange (MO) were selected as representative cationic and anionic dye pollutants, respectively. The adsorption isotherms and kinetics of MB and MO on the prepared adsorbents were examined at 25°C and pH 6.5–7. The prepared adsorbents (50 mg) were separately added to aqueous solutions containing the dyes at concentrations ranging from 1 to 10 mg/L. The solutions were placed in 50 mL amber bottles and stirred on a shaker table operated at 500 strokes/min for 6 h. For the kinetic study, a dye concentration of 10 ppm was prepared. Aliquots (1 mL) of the solutions were withdrawn at 1 min intervals and filtered through a polytetrafluoroethylene filter (pore size of 0.2 μm, Millipore, Chicago, IL, USA). The dye concentration was determined via ultraviolet-visible spectroscopy (Genesys 6, Thermo Spectronic, Rochester, NY, USA).

2.4 Adsorption isotherm and kinetic models

To assess dye adsorption, methylene blue (MB) and methyl orange (MO) To examine dye adsorption on the prepared adsorbents, the following equation was used (Rodwihok *et al*. 2021b, Supelano *et al*. 2020):

$$q_e = \frac{(c_0 - c_e)V}{m} \tag{1}$$

where c_0 and c_e ($mg \cdot g^{-1}$) are the initial and equilibrium concentrations of the dye, respectively, V (mL) is the volume of the dye solution, and m (g) is the mass of the adsorbent. To determine the most favorable model for dye adsorption, the data were fitted to various nonlinear adsorption models, including the Langmuir, Freundlich, Temkin, and Koble–Corrigan adsorption isotherm models.

The Langmuir model is designed to characterize the adsorption of monolayer adsorbates onto homogeneous adsorbent surfaces. Based on this model, the adsorbent sites possess uniform energy and each adsorbate molecule is exclusively localized at a single site. The nonlinear Langmuir isotherm is expressed as follows (Supelano *et al*. 2020):

$$q_e = \frac{(q_m K_L c_e)}{(1 + K_L c_e)} \quad (2)$$

where q_e ($mg \cdot g^{-1}$) represents the maximum monolayer adsorption capacity, and K_L (mL·g^{-1}) is the Langmuir constant, which is associated with the energy change during the adsorption process.

In contrast to the Langmuir model, the Freundlich model is not restricted to monolayer adsorption. It can be used to describe non-ideal adsorption characteristics, including those reflecting the presence of a heterogeneous adsorbent surface. The nonlinear Freundlich isotherm is expressed as follows (Ayawei *et al*. 2017, Supelano *et al*. 2020):

$$q_e = K_F c_e^{1/n_F} \quad (3)$$

where n_F represents the adsorption intensity, and K_F ($mg \cdot g^{-1}$) is the Freundlich constant, which is associated with the adsorption capacity.

The Kobble–Corrigan model is a combination of the Langmuir and Freundlich isotherm models and is designed to describe equilibrium adsorption data. This isotherm model incorporates an exponential function that relies on the concentrations expressed in both the numerator and denominator, which are typically employed to consider the effects of heterogeneous surfaces. The equation for the nonlinear Koble–Corrigan isotherm is expressed as follows (Rodwihok *et al*. 2021b, Supelano *et al*. 2020):

$$q_e = \frac{(A c_e^{n_K})}{(1 + B c_e^{n_K})} \quad (4)$$

where A ($L^{n_K} \cdot mg^{1-n_K} \cdot g^{-1}$) and B ($L^{n_K} \cdot mg^{-n_K}$) represent the Kobble–Corrigan isotherm constants, and *nK* represents the adsorption intensity.

To further understand the adsorption characteristics of the prepared adsorbents, the kinetic adsorption of the dye was examined as a function of the amount of dye adsorbed (q_t) at the contact time (min), which can be expressed as follows (Agbovi and Wilson 2021):

$$q_t = \frac{(c_0 - c_t)V}{m} \quad (5)$$

where c_t ($mg \cdot g^{-1}$) is the dye concentrations at contact time (min). The chemisorption mechanisms of the underlying processes were determined using nonlinear pseudo-first-order and second-order kinetic models. The nonlinear pseudo-first- and second-order kinetic models are expressed as follows (Agbovi and Wilson 2021):

Nonlinear pseudo first-order kinetic model:

$$q_t = q_{e1}(1 - e^{-k_1 t}) \quad (6)$$

Nonlinear pseudo second-order kinetic model:

$$q_t = \frac{(k_2 q_{e2}^2 t)}{(1 + k_2 q_{e2} t)} \quad (7)$$

where k_1 (min^{-1}) and k_2 ($g \cdot (mg \cdot min)^{-1}$) represent the adsorption rate constant of the pseudo first-order and second-order kinetic models, respectively, and q_{e1} and q_{e2} represent the adsorbed amounts of dye at equilibrium ($mg \cdot g^{-1}$).

The removal efficiency (R%) of MB and MO is calculated as follows:

$$R\% = [(q_0 - q_t)/q_0] \times 100 \quad (8)$$

3. Results and discussion

3.1 Preparation of zeolite/Zn adsorbents

FE-SEM analysis was performed to characterize the surfaces of CA, zeolite, and zeolite/Zn adsorbents. Well-defined and smooth spherical particles were observed on the surfaces of CA, whose sizes ranged from 0.83 to 4.54 μm, as shown in Fig. 1(a). Meanwhile, the zeolite exhibited a ferrospherical shape with microfissures, which is attributable to zeolization resulting from NaOH activation (Fig. 1(b)). The zeolite/Zn adsorbents showed a microporous ferrospherical shape with a cluster of miniscule particles (diameter less than 1 μm) dispersed throughout the entire surface (Fig. 1(c)). XRD analysis was conducted to investigate the crystal structures of the prepared adsorbents, and the results are shown in Fig. 1(d). The CA, zeolite, and zeolite/Zn exhibited similar XRD patterns, which corresponded to the mineralogical compositions of quartz Q (JCPDS:00-046-1045) and mullite-M (JCPDS:01-079-1275; Supelano *et al*. 2020). Upon the activation of CA using NaOH (A-CA), new diffraction peaks corresponding to cancrinite (ICSD:20334) and analcime (JCPDS:01-076-0143) were observed. Furthermore, CA activated using NaOH and zinc acetate (A-CA/Zn) showed similar XRD patterns but with additional diffraction peaks at 2θ = 31.8° and 34.4°, which corresponded to the (100) and (002) reflection planes of the ZnO hexagonal wurtzite structure, respectively (JCPDS:89-13971; Rodwihok *et al*. 2023). The size of a ZnO crystal can be calculated using the Scherrer equation as follows (Mote *et al*. 2012, Rodwihok *et al*. 2021a):

$$D = (K\lambda)/(\beta \cos\theta) \quad (9)$$

where D is the crystal size, K a dimensionless shape factor, λ the X-ray wavelength, β the broadening at one-half the maximum intensity, and θ the Bragg angle. The average ZnO crystal size of the zeolite/Zn was approximately 22.27 nm. These results were consistent with those shown by the FE-SEM images, i.e., ZnO particle clusters were dispersed on the zeolite surface.

To determine the physical adsorption capacity of the prepared adsorbents, nitrogen adsorption–desorption isotherm analyses using a BET surface analyzer were performed; subsequently, the specific pore volume and surface area were calculated, as presented in Table 1. The surface area of CA was determined to be 2.111 m^2·g^{-1}. However, after NaOH activation (zeolite), the surface area increased significantly to 15.785 m^2·g^{-1}, which indicates the generation of new micro/nanopores via zeolization. By contrast, the zeolite/Zn composites exhibited a lower surface area of 10.52 m^2·g^{-1} compared with zeolite. This reduction in the surface area was attributed to both zeolization and the formation of ZnO. In addition, the

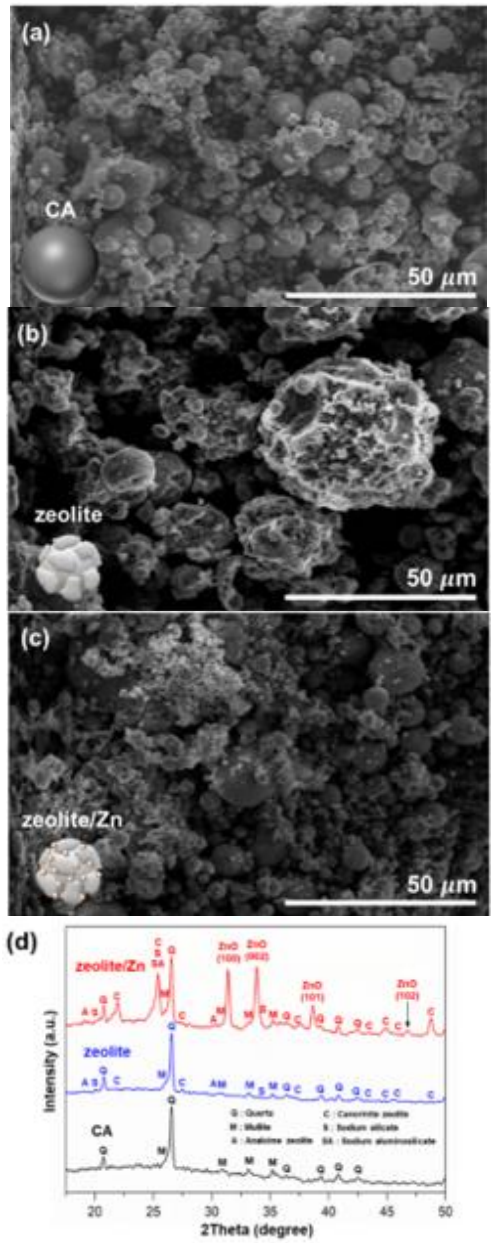

Fig. 1 FE-SEM images of (a) CA, (b) zeolite and (c) zeolite/Zn adsorbents, and their (d) XRD patterns

amount of Zn significantly decreased the surface area. Surface area is an important factor that affects the sorptive capacity; therefore, a large surface area provides more active adsorption sites (Visa *et al*. 2015b). Consequently, the increased surface area improves the adsorption capacity of the zeolite nanocomposites. Figs. 2(a) and (b) show the surface functionalization and zeta potentials of the adsorbents. As summarized in Table 1, the zeta potential of CA was initially negative (-13.40 eV), which further decreased after NaOH activation (-19.85 eV). When zinc acetate was added, the values became more negative (-24.32 eV). This appeared to be due to an increase in the number of OH groups on the surface of the adsorbent after NaOH and Zn activation, which can promote the electrostatic interaction between the adsorbents and dye molecules, thus improving dye removal by adsorption.

Table 1 Pore structure and surface charge properties

Adsorbents	CA	zeolite	zeolite/Zn
V_{BET} ($10^{-3} \cdot cm^3 \cdot g^{-1}$)	3.76	52.45	39.90
S_{BET} ($m^2 \cdot g^{-1}$)	2.11	15.78	10.52
Zeta potential (eV)	-13.40	-19.85	-24.32

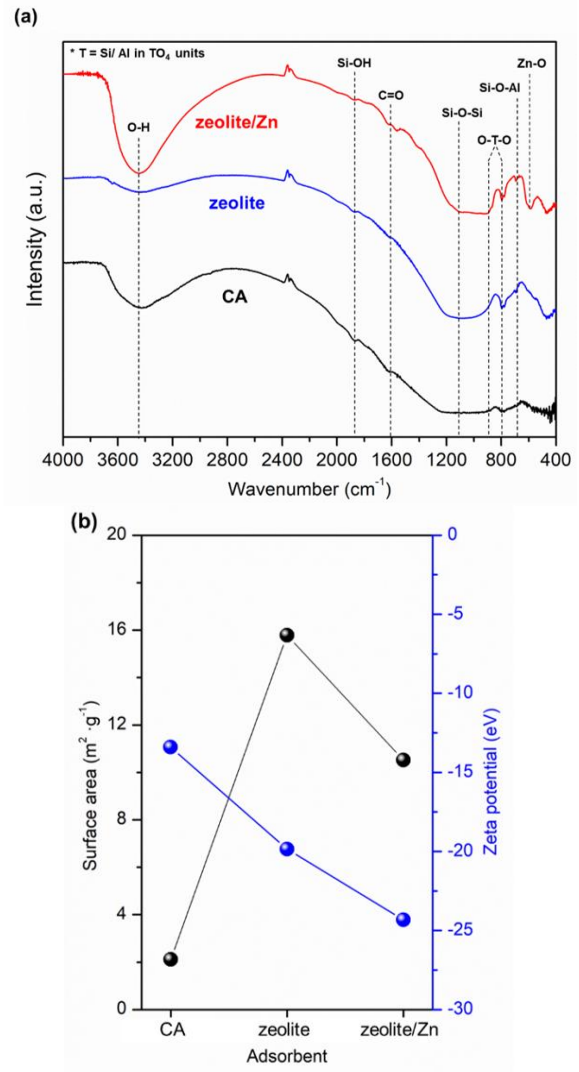

Fig. 2 (a) FT-IR spectra and (b) zeta potential (in eV) of prepared adsorbents

3.2 MB and MO adsorption onto zeolite/Zn adsorbents

3.2.1 Adsorption isotherms

The MB and MO adsorption isotherms were analyzed using nonlinear adsorption models, as depicted in Fig. 3. The adsorption isotherm parameters are presented in Table 2. The data of MB and MO adsorption onto CA fitted well with the Langmuir isotherm model, with high correlation coefficients (r^2) of 0.985 and 0.997, respectively, as compared with those of the other models. This suggests that the Langmuir isotherm model is the most suitable model for describing the adsorption of MB and MO molecules on CA (Rodwihok *et al*. 2023). By contrast, their adsorption onto

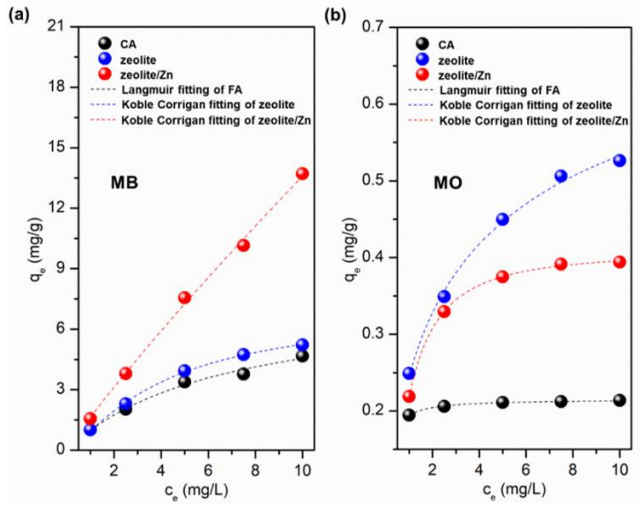

Fig. 3 Adsorption isotherms for (a) MB and (b) MO (Dashed lines indicate adsorption isotherm model fits.)

zeolite and zeolite/Zn composites indicated the highest r^2 values under the Kobble–Corrigan isotherm model. Therefore, this model is the most appropriate for describing the adsorption of MB and MO onto the abovementioned nanocomposites, i.e., it occurred via monolayer and multilayer coverage mechanisms (Ayawei *et al*. 2017)

3.2.2 Adsorption kinetics

The adsorption kinetics were examined using nonlinear pseudo-first- and second-order kinetic models, as shown in Fig. 4. The parameters and correlation coefficients were calculated using the OriginPro 8.5 software (Northampton, MA, USA). Table 2 provides comparative analysis data for the equilibrium adsorption quantities of MB and MO. The nonlinear pseudo-first-order model explained the experimental adsorption data for MB and MO well, thus supporting the significance of chemical interactions on the adsorption process. In addition, the nonlinear pseudo-first-order kinetic model was suitable for describing the adsorption of MB and MO. The adsorption of the dye molecules occurred in a two-step process, as depicted in Fig. 4. Initially, a rapid adsorption phase occurred, which was ascribed to diffusion in the boundary layer. During this phase, the dye molecules migrated to the external surface of the adsorbent and were adsorbed. This process appeared to be affected by the molecular diffusion properties, presence of activated adsorption sites, and specific surface area of the adsorbents. Subsequently, slower adsorption occurred, which was characterized by the internal diffusion of the dye molecules within the porous structure of the adsorbents. As the MB and MO molecules penetrated the pores, they were gradually absorbed into the internal pore structure until equilibrium was attained (Rodwihok *et al*. 2023, Zafar *et al*. 2019).

3.3 Enhancement in selective adsorption mechanisms

The dye removal efficiency by adsorption was determined, and the results are listed in Table 2. MB can be adsorbed onto the surface of CA, zeolite, and zeolite/Zn

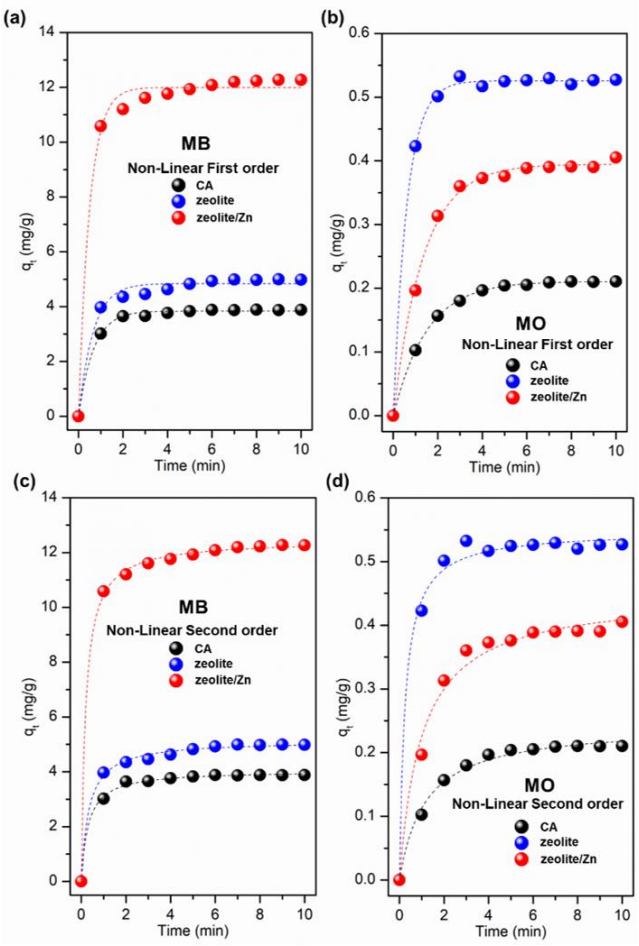

Fig. 4 Kinetic models for adsorption of MB and MO: (a and b) nonlinear pseudo-first-order model and (c and d) nonlinear pseudo-second-order model

adsorbents better than MO (Fig. 5(a)). These results indicate that the electrostatic interactions between the adsorbents and dye molecules significantly affect the selective adsorption capacity of the dyes, as shown in Fig. 5(b). CA, zeolite, and zeolite/Zn adsorbents, which possess negative zeta potentials, exhibit high selectivity for MB over MO. During the adsorption process, MB (cationic dye) was favorably adsorbed because of the electrostatic attraction between the positively charged $=NH^+$ group (positive dipole) of MB and the negatively charged surface of the adsorbents (Basha *et al*. 2022, Molla *et al*. 2019). Among the adsorbents, zeolite/Zn, which has a more negative zeta potential, demonstrated a higher MB removal efficiency by adsorption onto CA and zeolite. However, MO (an anionic dye) contributed less effectively to the adsorption process because of the electrostatic repulsion between the negatively charged oxygen functional group (negative dipole) of MO and the negative surface charge of the adsorbents. However, the adsorbents with larger surface areas exhibited higher MO removal efficiencies. During the synthesis of zeolite/Zn, approximately 3.14 g of dried zeolite/Zn can be obtained in 100 ml Teflon-lined autoclave and the price per gram can be calculated as 0.0171 USD/g zeolite/Zn, which costs less than for the conventional absorbents (Praveen *et al*. 2021). This suggests that the

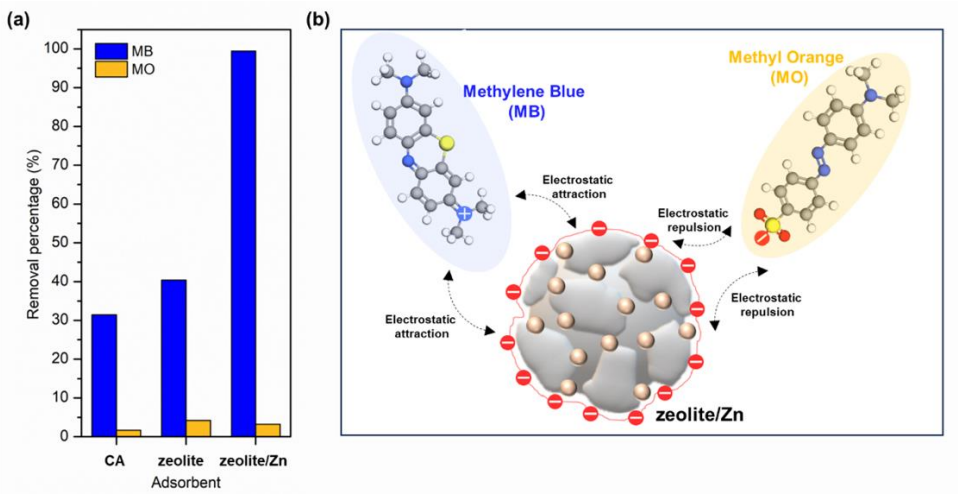

Fig. 5 (a) Removal efficiencies of MB and MO and (b) adsorption process of MB and MO onto zeolite/Zn adsorbent

Table 2 Parameters for adsorption isotherms and adsorption kinetics

Adsorbents	CA		zeolite		zeolite/Zn	
Dye type	MB	MO	MB	MO	MB	MO
Adsorption isotherm model						
Langmuir model						
K_L (mL · g^{-1})	0.148	9.153	0.142	0.615	0.016	1.064
q_m (mg · g^{-1})	7.608	0.216	9.074	0.606	95.400	0.440
r^2	0.985	0.997	0.993	0.980	0.996	0.985
Freundlich model						
K_F (mg · g^{-1})	1.169	0.196	1.321	0.259	1.666	0.247
n_F	1.660	25.141	1.620	3.115	1.096	4.430
r^2	0.977	0.926	0.966	0.982	0.997	0.858
Koble–Corrigan model						
A (L^n_K · mg$^{1-n}_K$ · g^{-1})	1.155	1.847	1.109	0.353	1.648	0.470
B (L^n_K · mg$^{-n}_K$)	0.137	8.492	0.159	0.436	0.005	1.147
n_K	0.936	0.814	1.282	0.645	0.934	1.400
r^2	0.978	0.996	0.998	0.993	0.998	0.999
Adsorption kinetic model						
Experimental adsorption capacity (q_{exp}) (mg · g^{-1})	3.870	0.208	4.951	0.526	12.163	0.390
Nonlinear pseudo-first order						
q_{e1} (mg · g^{-1})	3.840	0.211	4.842	0.526	11.995	0.394
k_1 (min^{-1})	1.511	0.668	1.538	1.627	2.024	0.742
r^2	0.997	0.999	0.992	0.999	0.990	0.997
Nonlinear pseudo-second order						
q_{e2} (mg · g^{-1})	4.046	0.243	5.139	0.548	12.451	0.449
k_2 (g · (mg · min)$^{-1}$)	0.808	3.594	0.589	7.356	0.419	2.238
r^2	0.997	0.992	0.996	0.994	0.997	0.985
Removal percentage (%)	31.45	1.68	40.38	4.21	99.41	3.24

alkali/Zn surface modification with CA can improve the surface properties (surface area and negative charge), resulting in enhancement in adsorption capacity and selectivity for dyes and reusability of CA.

4. Conclusions

In this study, a simple hydrothermal method using NaOH and Zn was employed to synthesize a zeolite-based

adsorbent composite based on CA. The CA-derived zeolite exhibited excellent adsorption properties as an effective and selective adsorbent for organic dye pollutants. The activation of CA-derived zeolites using NaOH and Zn resulted in the formation of materials with larger surface areas and enhanced negative surface charges. The zeolite/Zn composite showed a negative zeta potential, thus rendering it highly effective in selectively adsorbing cationic dye molecules, such as MB, via favorable electrostatic interactions between the positive dipole of the $=NH^+$ group in the MB molecules and the oxygen functional group in the zeolite/Zn adsorbent. Conversely, anionic dyes, such as MO, exhibited relatively ineffective absorption, thus highlighting the preferential affinity of the zeolite/Zn adsorbent for cationic dyes. These findings emphasize the significant role of electrostatic interactions in the adsorption process, in addition to the effect of surface area. It is to be noted that the removal efficiency can be different depending on the affinity characteristics between adsorbents and adsorbates.

Acknowledgments

This study was supported by the National Research Foundation of Korea grant funded by the Korea Ministry of Science and ICT (2022R1I1A1A01056866122068207325010 2 and RS-2023-00208933206820732500 01), the Seoul Green Environmental Center (202303500001), and the Konkuk University Research Support Program for the Faculty Sabbatical in 2021.

References

Agbovi, H.K., Wilson, L.D. (2021), "Adsorption processes in biopolymer systems: fundamentals to practical applications", in *Natural Polymers-Based Green Adsorbents for Water Treatment*, Elsevier.

Ahmad, T., Pandey, V., Husain, S.M., Adiba, Munjal, S. (2022), "Structural and spectroscopic analysis of pure phase hexagonal wurtzite ZnO nanoparticles synthesized by sol-gel. Mater", *Today Proc*., **49**, 1694-1697. https://doi.org/10.1016/j.matpr.2021.07.456

Al-Tohamy, R., Ali, S.S., Li, F., Okasha, K.M., Mahmoud, Y.A.-G., Elsamahy, T., Jiao, H., Fu, Y., Sun, J. (2022), "A critical review on the treatment of dye-containing wastewater: Ecotoxicological and health concerns of textile dyes and possible remediation approaches for environmental safety", *Ecotoxicol. Environ. Safe*., **231**, 113160. https://doi.org/10.1016/j.ecoenv.2021.113160

Ayawei, N., Ebelegi, A.N., Wankasi, D. (2017), "Modelling and interpretation of adsorption isotherms", *J. Chem*., 3039817. https://doi.org/10.1155/2017/3039817

Balintova, M., Kovacova, Z., Demcak, S., Chernysh, Y., Junakova, N. (2021), "Comparison of sorption efficiency of natural and MnO2 coated zeolite for copper removal from model solutions", *Proceedings of the OP Conference Series: Earth and Environmental Science*, **900**(1), 12003. https://doi.org/10.1088/1755-1315/900/1/012003

Basha, I.K., Abd El-Monaem, E.M., Khalifa, R.E., Omer, A.M., Eltaweil, A.S. (2022), "Sulfonated graphene oxide impregnated cellulose acetate floated beads for adsorption of methylene blue dye: Optimization using response surface methodology", *Sci. Rep*., **12**, 9339. https://doi.org/10.1038/s41598-022-13105-4

Zol, M.N.B., Shuhaim, M.F.B., Yu1c, J., Lim, Y., Choe, J.W., Bae, S. and Kim, H. S. (2020), "Immobilization of oxidative enzymes onto Cu-activated zeolite to catalyze 4-chlorophenol decomposition", *Membr. Water Treat*., **11**(3), 195-200. https://doi.org/10.12989/MWT.2020.11.3.195

David, P.S., Karunanithi, A., Fathima, N.N. (2020), "Improved filtration for dye removal using keratin-polyamide blend nanofibrous membranes", *Environ. Sci. Pollut. Res*., **27**, 45629-45638. https://doi.org/10.1007/s11356-020-10491-y

He, X., Yang, D.P., Zhang, X., Liu, M., Kang, Z., Lin, C., Jia, N., Luque, R. (2019), "Waste eggshell membrane-templated CuO-ZnO nanocomposites with enhanced adsorption, catalysis and antibacterial properties for water purification", *Chem. Eng. J*., **369**, 621-633. https://doi.org/10.1016/j.cej.2019.03.047

Ihaddaden, S., Aberkane, D., Boukerroui, A., Robert, D. (2022), "Removal of methylene blue (basic dye) by coagulation-flocculation with biomaterials (bentonite and Opuntia ficus indica)", *J. Water Proc. Eng*., **49**, 102952. https://doi.org/10.1016/j.jwpe.2022.102952

Januário, E.F.D., Vidovix, T.B., Bergamasco, R., Vieira, A.M.S. (2021), "Performance of a hybrid coagulation/flocculation process followed by modified microfiltration membranes for the removal of solophenyl blue dye", *Chem. Eng. Proc*., **168**, 108577. https://doi.org/10.1016/j.cep.2021.108577

Jawad, A.H., Abdulhameed, A.S., Reghioua, A., Yaseen, Z.M. (2020), "Zwitterion composite chitosan-epichlorohydrin/zeolite for adsorption of methylene blue and reactive red 120 dyes", *Int. J. Biol. Macromol*., **163**, 756-765. https://doi.org/10.1016/j.ijbiomac.2020.07.014

Joseph, J., Radhakrishnan, R.C., Johnson, J.K., Joy, S.P., Thomas, J. (2020), "Ion-exchange mediated removal of cationic dye-stuffs from water using ammonium phosphomolybdate", *Mater. Chem. Phys*., **242**, 122488. https://doi.org/10.1016/j.matchemphys.2019.122488

Kaur, P., Rajani, N., Kumawat, P., Singh, N., Kushwaha, J.P. (2018), "Performance and mechanism of dye extraction from aqueous solution using synthesized deep eutectic solvents", *Colloids Surf. A*, **539**, 85-91. https://doi.org/10.1016/j.colsurfa.2017.12.013

Kazemi, J., Javanbakht, V. (2020), "Alginate beads impregnated with magnetic Chitosan@Zeolite nanocomposite for cationic methylene blue dye removal from aqueous solution", *Int. J. Biol. Macromol*., **154**, 1426-1437. https://doi.org/10.1016/j.ijbiomac.2019.11.024

Lee, W.K.W., van Deventer, J.S.J. (2003), "Use of infrared spectroscopy to study geopolymerization of heterogeneous amorphous aluminosilicates", *Langmuir*, **19**, 8726-8734. https://doi.org/10.1021/la026127e

Lellis, B., Fávaro-Polonio, C.Z., Pamphile, J.A., Polonio, J.C. (2019), "Effects of textile dyes on health and the environment and bioremediation potential of living organisms", *Biotechnol. Res. Innov*., **3**, 275-290. https://doi.org/10.1016/j.biori.2019.09.001

Li, C.J., Zhang, Y.J., Chen, H., He, P.Y., Zhang, Y., Meng, Q. (2021), "Synthesis of fly ash cenospheres-based hollow ABW zeolite for dye removal via the coupling of adsorption and photocatalysis", *Adv. Powder Technol*., **32**, 3436-3446. https://doi.org/10.1016/j.apt.2021.07.029

Li, H., Zheng, F., Wang, J., Zhou, J., Huang, X., Chen, L., Hu, P., Gao, J., Zhen, Q., Bashir, S., Liu, J.L. (2020), "Facile preparation of zeolite-activated carbon composite from coal gangue with enhanced adsorption performance", *Chem. Eng. J*., **390**, 124513. https://doi.org/10.1016/j.cej.2020.124513

Li, K.M., Jiang, J.G., Tian, S.C., Chen, X.J., Yan, F. (2014), "Influence of silica types on synthesis and performance of

amine-silica hybrid materials used for CO2 capture", *J. Phys. Chem. C*, **118**, 2454-2462. https://doi.org/10.1021/jp408354r

Lim, J.M., Park, J., Park, J.T., Bae, S. (2019), "Preparation of quasi-solid-state electrolytes using a coal fly ash derived zeolite-X and -A for dye-sensitized solar cells", *J. Ind. Eng. Chem.*, **71**, 378-386. https://doi.org/10.1016/j.jiec.2018.11.049

Lim, Y., Yu, J., Park, S., Kim, M., Chen, S., Bakri, N.A.B., Sabri, N.I.A.B.M., Bae, S., Kim, H.S. (2020), "Development of biocatalysts immobilized on coal ash-derived Ni-zeolite for facilitating 4-chlorophenol degradation", *Bioresour Technol.*, **307**, 123201. https://doi.org/10.1016/j.biortech.2020.123201

Lin, L., Lin, Y., Li, C., Wu, D., Kong, H. (2016), "Synthesis of zeolite/hydrous metal oxide composites from coal fly ash as efficient adsorbents for removal of methylene blue from water", *Int. J. Miner. Proc.*, **148**, 32-40. https://doi.org/10.1016/j.minpro.2016.01.010

Madan, S., Shaw, R., Tiwari, S., Tiwari, S.K. (2019), "Adsorption dynamics of Congo red dye removal using ZnO functionalized high silica zeolitic particles", *Appl. Surf. Sci.*, **487**, 907-917. https://doi.org/10.1016/j.apsusc.2019.04.273

Molla, A., Li, Y., Mandal, B., Kang, S.G., Hur, S.H., Chung, J.S. (2019), "Selective adsorption of organic dyes on graphene oxide: Theoretical and experimental analysis", *Appl. Surf. Sci.*, **464**, 170-177. https://doi.org/10.1016/j.apsusc.2018.09.056

Mote, V.D., Huse, V.R., Purushotham, Y., Shah, S.S., Dole, B.N. (2012), "Synthesis and characterization of Mn doped ZnS nanometer-sized particles", *AIP Conf. Proc.*, **1447**, 217-218. https://doi.org/10.1063/1.4709957

Nyankson, E., Adjasoo, J., Efavi, J.K., Yaya, A., Manu, G., Kingsford, A., Abrokwah, R.Y. (2020), "Synthesis and kinetic adsorption characteristics of Zeolite/CeO2 nanocomposite", *Sci. African*, **7**, e00257. https://doi.org/10.1016/j.sciaf.2019.e00257

Park, J., Hwang, Y., Bae, S. (2019), "Nitrate reduction on surface of Pd/Sn catalysts supported by coal fly ash-derived zeolites", *J. Hazard. Mater.*, **374**, 309-318. https://doi.org/10.1016/j.jhazmat.2019.04.051

Park, S., Kim, M., Lim, Y., Yu, J., Chen, S., Woo, S.W., Yoon, S., Bae, S., Kim, H.S. (2021), "Characterization of rare earth elements present in coal ash by sequential extraction", J. *Hazard. Mater.*, **402**, 123760. https://doi.org/10.1016/j.jhazmat.2020.123760

Praveen, S., Gokulan, R., Pushpa, T.B., Jegan, J. (2021), "Techno-economic feasibility of biochar as biosorbent for basic dye sequestration", *J. Indian Chem. Soc.*, **98**, 100107. https://doi.org/https://doi.org/10.1016/j.jics.2021.100107

Querol, X., Moreno, N., Umaña, J.C., Alastuey, A., Hernández, E., López-Soler, A., Plana, F. (2002), "Synthesis of zeolites from coal fly ash: an overview", *Int. J. Coal Geol.*, **50**, 413-423. https://doi.org/10.1016/S0166-5162(02)00124-6

Rakanović, M., Vukojević, A., Savanović, M.M., Armaković, S., Pelemiš, S., Živić, F., Sladojević, S., Armaković, S.J. (2022), "Zeolites as adsorbents and photocatalysts for removal of dyes from the aqueous environment", *Molecules*, **27**(19), 6582. https://doi.org/10.3390/molecules27196582

Rodwihok, C., Charoensri, K., Wongratanaphisan, D., Choi, W.M., Hur, S.H., Park, H.J., Chung, J.S. (2021a), "Improved photocatalytic activity of surface charge functionalized ZnO nanoparticles using aniline", *J. Mater. Sci. Technol.*, **76**, 1-10. https://doi.org/10.1016/j.jmst.2020.09.041

Rodwihok, C., Suwannakaew, M., Han, S.W., Lim, Y.J., Park, S.Y., Woo, S.W., Choe, J.W., Wongratanaphisan, D., Kim, H.S. (2023), "Effective removal of hazardous organic contaminant using integrated photocatalytic adsorbents: Ternary zinc oxide/ zeolite-coal fly ash/reduced graphene oxide nanocomposites", *Colloids Surf. A*, **662**, 131044. https://doi.org/10.1016/j.colsurfa.2023.131044

Rodwihok, C., Suwannakeaw, M., Charoensri, K., Wongratanaphisan, D., Woon Woo, S., Kim, H.S. (2021b), "Alkali/zinc-activated fly ash nanocomposites for dye removal and antibacterial applications", *Bioresour. Technol.*, **331**, 125060. https://doi.org/10.1016/j.biortech.2021.125060

Rubab, M., Bhatti, I.A., Nadeem, N., Shah, S.A.R., Yaseen, M., Naz, M.Y., Zahid, M. (2021), "Synthesis and photocatalytic degradation of rhodamine B using ternary zeolite/WO3/Fe3O4 composite", *Nanotechnology*, **32**, 345705. https://doi.org/10.1088/1361-6528/ac037f

Saruchi, Kumar, V. (2019), "Adsorption kinetics and isotherms for the removal of rhodamine B dye and Pb+2 ions from aqueous solutions by a hybrid ion-exchanger", *Arab. J. Chem.*, **12**, 316-329. https://doi.org/10.1016/j.arabjc.2016.11.009

Shui, Z., Yao, L., Pu, X., Yang, L., Jiang, W., Jiang, X. (2020), "Synthesis of a novel zeolite-activated carbon composite using lithium-silicon-powder waste for ammonia-nitrogen and methylene blue removal", *Ind. Eng. Chem. Res.*, **59**, 14616-14624. https://doi.org/10.1021/acs.iecr.0c00617

Singh, N.J., Wareppam, B., Kumar, A., Singh, K.P., Garg, V.K., Oliveira, A.C., Singh, L.H. (2023), "Zeolite incorporated iron oxide nanoparticle composites for enhanced congo red dye removal", *J. Mater. Res.*, **38**, 1149-1161. https://doi.org/10.1557/s43578-022-00859-w

Supelano, G.I., Gómez Cuaspud, J.A., Moreno-Aldana, L.C., Ortiz, C., Trujillo, C.A., Palacio, C.A., Parra Vargas, C.A., Mejía Gómez, J.A. (2020), "Synthesis of magnetic zeolites from recycled fly ash for adsorption of methylene blue", *Fuel*, **263**, 116800. https://doi.org/10.1016/j.fuel.2019.116800

Visa, M., Andronic, L., Duta, A. (2015a), "Fly ash-TiO2 nanocomposite material for multi-pollutants wastewater treatment", *J. Environ. Manage.*, **150**, 336-343. https://doi.org/10.1016/j.jenvman.2014.10.026

Visa, M., Bogatu, C., Duta, A. (2015b), "Tungsten oxide - fly ash oxide composites in adsorption and photocatalysis", *J. Hazard. Mater.*, **289**, 244-256. https://doi.org/10.1016/j.jhazmat.2015.01.053

Wang, X., Jiang, J., Gao, W. (2022), "Reviewing textile wastewater produced by industries: characteristics, environmental impacts, and treatment strategies", *Water Sci. Technol.*, **85**, 2076-2096. https://doi.org/10.2166/wst.2022.088

Zafar, M.N., Dar, Q., Nawaz, F., Zafar, M.N., Iqbal, M. and Nazar, M.F. (2019), "Effective removal of azo dyes over spherical ZnO nanoparticles", *J. Mater. Res. Technol.*, **8**, 713-725. https://doi.org/10.1016/j.jmrt.2018.06.002

Zhang, Y., Tang, Q., Chen, S., Gu, F., Zhene, L. (2018), "Heavy metal adsorption of a novel membrane material derived from senescent leaves: Kinetic, equilibrium and thermodynamic studies", *Membr. Water Treat.*, **9**(2), 95-104. https://doi.org/10.12989/mwt.2018.9.2.095

Zol, M.N. Bin, Shuhaimi, M.F. Bin, Yu, J., Lim, Y., Choe, J.W., Bae, S., Kim, H.S. (2020), "Immobilization of oxidative enzymes onto Cu-activated zeolite to catalyze 4-chlorophenol decomposition", *Membr. Water Treat.*, **11**(3), 195-200. https://doi.org/10.12989/mwt.2020.11.3.195

YH